

## CHAPTER IV

### EXPERIMENTS AND RESULTS

The experiments were conducted to form the proton tracks on PC under various conditions to estimate the correlation between the track density, average track size and the percentage of light transmission in three ranges i.e. ultraviolet, visible light and infrared. Track density was varied by varying irradiation time and track size and shape were controlled by etching temperature and etching time.

#### 4.1 Formation of proton tracks using thermal neutrons from the Thai Research Reactor

This first step was to investigate proton track formation on PC, the effects of etching temperature and etching time. Four pieces of 2.5 cm x 5 cm PC chips were irradiated with neutrons from a beam tube designed for neutron radiography at the Thai Research Reactor TRR-1/M1 (Figure 4.1) for 1 hour. The neutron flux was approximately  $1.26 \times 10^6$  n/cm<sup>2</sup>.s with a cadmium ratio of greater than 200 [30]. PEW solution containing 15% potassium hydroxide (KOH), 40% ethyl alcohol (C<sub>2</sub>H<sub>5</sub>OH) and 45 % water (H<sub>2</sub>O) was selected as the etchant. The neutron irradiated PC chips were then etched separately at different temperatures i.e. 65, 70, 75 and 80 °C each for 60 minutes. The etched track images at different conditions were shown in Figures 4.2 - 4.3.

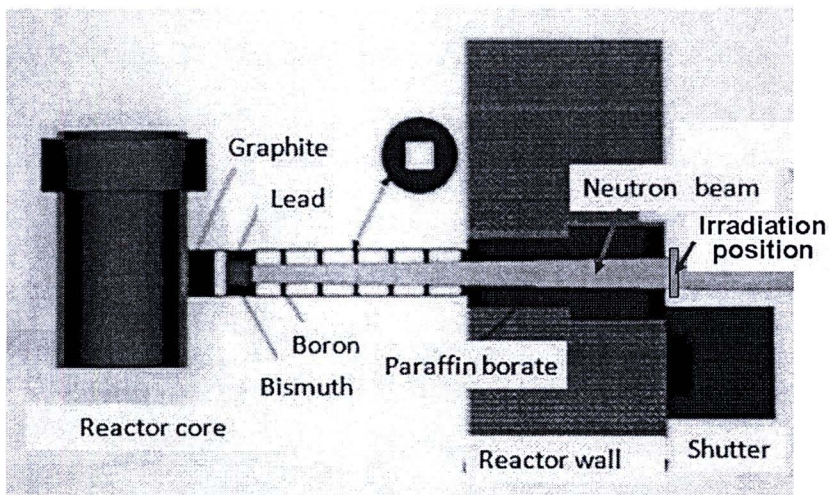


Figure 4.1 Diagram showing the thermal neutron beam for neutron radiography at the Thai Research Reactor TRR1/M1.

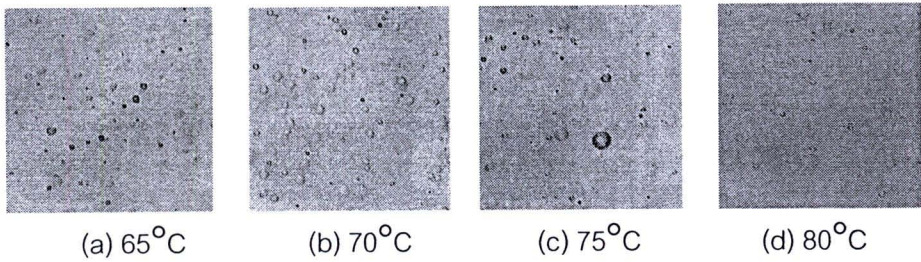


Figure 4.2 Proton track images on PC (x 100) at different etching temperatures.

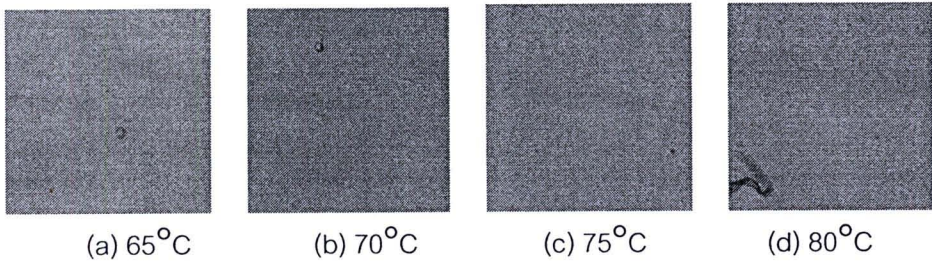


Figure 4.3 Unexposed PC images (x 100) after etching at different temperatures.

The track density of each etching temperature was shown in table 4.1. It showed that track density decreased with increasing of the etching temperature. This was because the etching rate at higher temperature was faster than at lower temperature. The etching time of 1 hour was too long for higher temperatures thus some of proton tracks nearer to the surface were already removed as could be clearly seen in Figure 4.2 from (a) to (d). Distribution of track diameter at different etching temperatures i.e. 65, 70, 75 and 80°C was also shown in Table 4.2 and Figure 4.4 - 4.7.

Table 4.1 Track densities at the different temperatures

Etching Temperature	Track density (tracks/ cm <sup>2</sup> )	Sensitivity in formation of proton tracks
65°C	$1.68 \times 10^5$	$3.70 \times 10^{-5}$
70°C	$1.56 \times 10^5$	$3.44 \times 10^{-5}$
75°C	$1.55 \times 10^5$	$3.41 \times 10^{-5}$
80°C	$1.30 \times 10^5$	$2.86 \times 10^{-5}$

For irradiation time of 1 hour, the neutron fluence or total neutrons at the irradiation position was approximately  $1.26 \times 10^6 \text{ n/cm}^2 \cdot \text{s} \times 3600 \text{ s} = 4.54 \times 10^9 \text{ n/cm}^2$ . The sensitivity of PC to neutrons from the research reactor in formation of recoil proton tracks could then be calculated. For example at  $65^\circ\text{C}$ , the sensitivity was  $(1.68 \times 10^5 \text{ tracks/cm}^2) \div (4.54 \times 10^9 \text{ n/cm}^2) = 3.7 \times 10^{-5}$ .

Table 4.2 Distribution of track diameter at different temperatures

Track diameter ( $\mu\text{m}$ )	Number of track in percentage (%)			
	$65^\circ\text{C}$	$70^\circ\text{C}$	$75^\circ\text{C}$	$80^\circ\text{C}$
2	8	3	2	3
3	18	7	2	11
4	16	9	6	10
5	19	8	14	8
6	19	21	20	15
7	17	16	18	19
8	4	12	16	6
9	8	9	10	8
10	3	7	9	4
11	4	8	1	2
12	1	6	4	2
13	5	4	1	2
14	0	2	2	3
15	0	1	5	1
16	0	0	2	1
17	0	0	1	0
18	0	0	1	0
>19	0	0	1	0

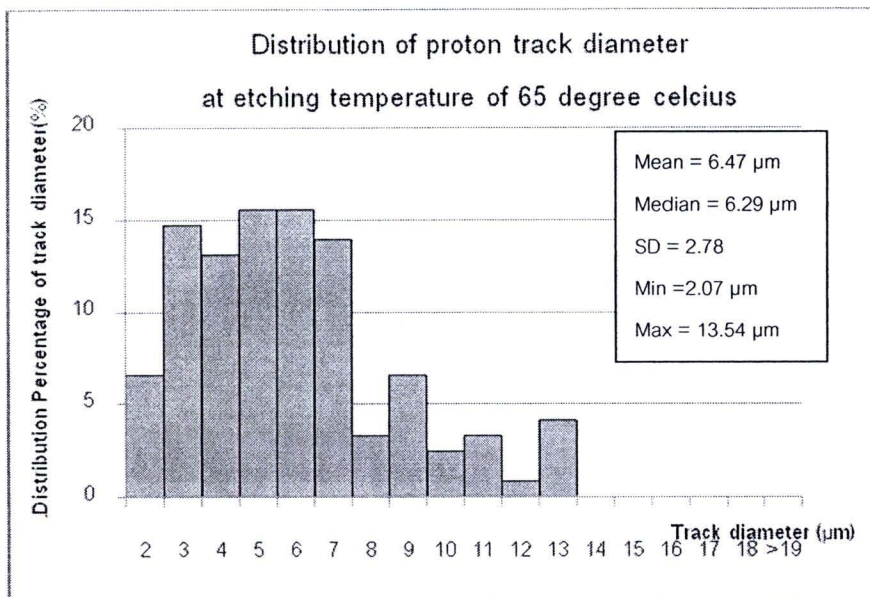


Figure 4.4 Distribution of track diameter at etching temperature 65°C.

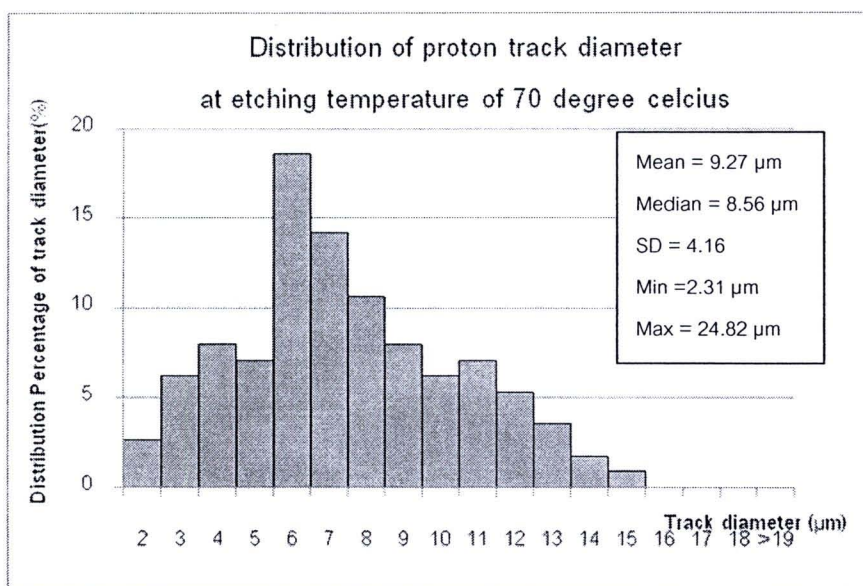


Figure 4.5 Distribution of track diameter at etching temperature 70°C.

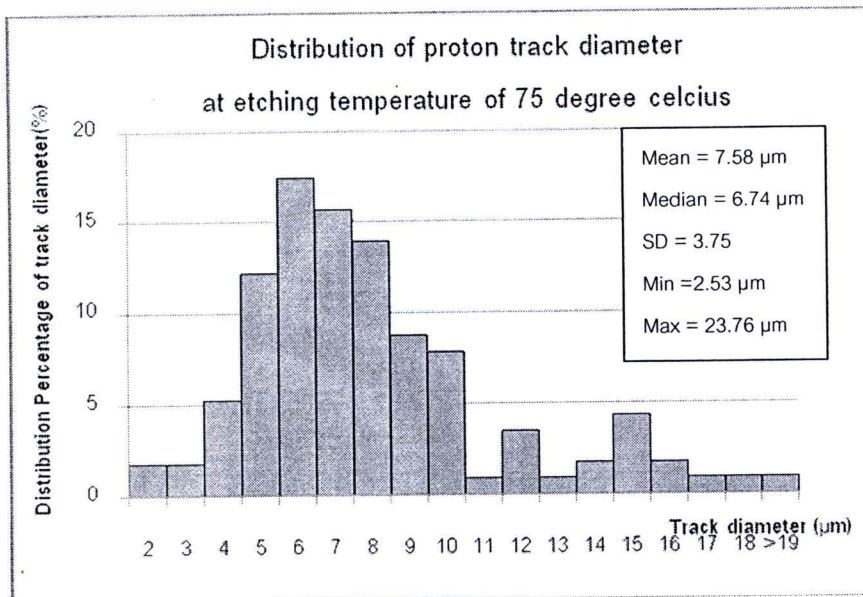


Figure 4.6 Distribuyion of track diameter at etching temperature 75°C.

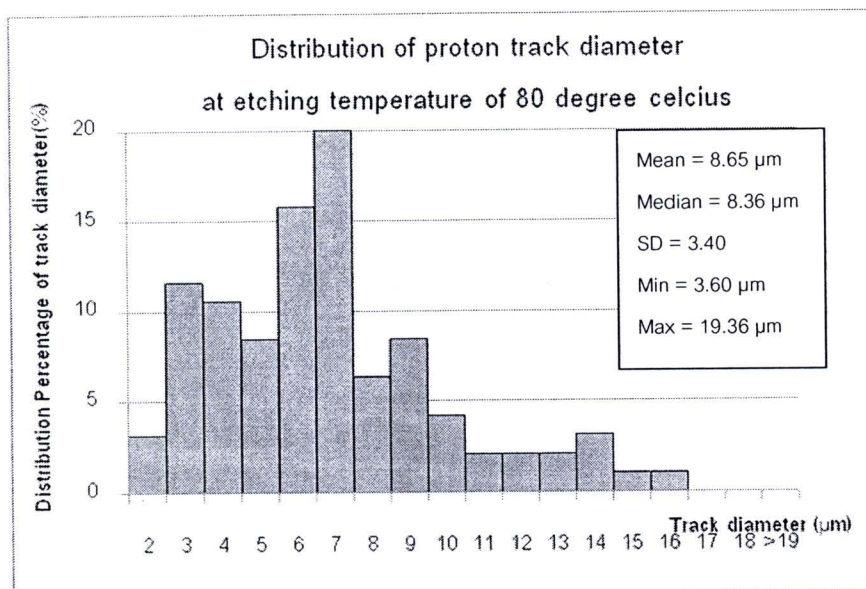


Figure 4.7 Distribution of track diameter at etching temperature 80°C.

Table 4.3 showed the mean, median, standard deviation (SD), minimum and maximum values of track diameter in each etching temperature.

Table 4.3 Track diameter statistics for each etching temperatures

Etching temperature	Track diameter ( $\mu\text{m}$ )				
	Mean	Median	SD	Minimum	Maximum
65 $^{\circ}\text{C}$	6.47	6.29	2.78	2.07	13.54
70 $^{\circ}\text{C}$	9.27	8.56	4.16	2.31	24.82
75 $^{\circ}\text{C}$	7.58	6.74	3.75	2.53	23.76
80 $^{\circ}\text{C}$	8.65	8.36	3.40	3.60	19.36

As illustrated in Figures 4.4 - 4.7, distribution of track diameter at the different etching temperatures was in similar pattern but different in track diameter particularly between 65 $^{\circ}\text{C}$  and other etching temperatures. The track diameters at the 65 $^{\circ}\text{C}$  were mainly in the range of 3 - 7 micrometers ( $\mu\text{m}$ ) while the mean and median of track diameter were 6.47  $\mu\text{m}$  and 6.29  $\mu\text{m}$  respectively. There was no track with the diameter greater than 15  $\mu\text{m}$ . Distribution of track diameter at 70, 75 and 80 $^{\circ}\text{C}$  etching temperatures was similar to at 65 $^{\circ}\text{C}$  but the average track diameters were larger.

Light transmission through PC in three regions, i.e. ultraviolet (UV), visible light and infrared (IR), were carried out by using a SPECTRUM DETECTIVE Transmission Meter SD2400 the results are shown in Table 4.4.

Table 4.4 Percentage of light transmission at the different temperatures

Light region	Percentage of transmission						
	No PC (Blank)	$C_{\text{no etch}}$	$C_{\text{etch}}$	65 $^{\circ}\text{C}$	70 $^{\circ}\text{C}$	75 $^{\circ}\text{C}$	80 $^{\circ}\text{C}$
UV	100	0	0	0	0	0	0
Light	100	85	85	76	79	77	80
IR	100	91	92	83	84	83	87

Note :  $C_{\text{no etch}}$  = unexposed PC without etching  
 $C_{\text{etch}}$  = unexposed PC etched at the 80 $^{\circ}\text{C}$  for 1 hr

The results showed that PC itself could completely absorb UV while 85 % of visible light and 92 % of IR could transmit through the etched-unexposed PC. This was due to inherent property of PC. For etched PC having recoil proton tracks, percentage of visible light and IR transmission decreased in comparison to the PC with no tracks. at 65, 70 and 75 °C were not different significantly. But the percentage of visible light transmission were different. Light transmitted track-etched PC at 65 °C less than the other conditions. The probably reason was the bigger number of track density. The percentage of visible light and IR transmission of PC at 80 °C was increased again due to some of tracks on the surface were removed.

#### 4.2 Formation of proton tracks using neutrons from a Cf-252 source

Californium-251 (<sup>252</sup>Cf) is a small sealed neutron source normally used for neutron activation analysis (NAA), neutron-induced prompt gamma-ray analysis, neutron radiography, moisture measurement, etc. It gives high neutron output, approximately  $2.3 \times 10^6$  neutrons/second per microgram, from spontaneous fission with a half-life of 2.6 years and the average neutron energy of 2 MeV [Appendix A]. It is most practical for use in producing track-etched PC as light filter and/or diffuser. This study is, therefore, focused on using a Cf-252 source. The source at the time of this investigation (June, 2010) had the neutron output of approximately  $5 \times 10^6$  n/s which gave maximum thermal neutron flux of about  $5 \times 10^4$  n/cm<sup>2</sup>.s in water from the source. Neutron flux at other distances is shown in Figure 3, Appendix A. Neutrons irradiation was carried out by placing 4 pieces of PC chips under water at a desired position. The neutron irradiated PC chips were then etched under various conditions and tested as in the previous experiment.

##### 4.2.1 Effects of etching temperature and etching time

Theoretically, formation of recoil proton tracks is dependent on neutron energy spectrum. As mentioned earlier, the cadmium ratio was about 200 for thermal neutrons from the neutron radiography tube at the nuclear reactor. For the Cf-252 source, it has been reported that the cadmium ratio was 10 – 20 [26] which was about 10 – 20 times lower. This means the average thermal neutron energy in water from the Cf-252 was higher. Formation of proton tracks and effects of etching temperature and etching time

may be in different degrees. Therefore, the experiment had to be repeated to investigate effects of etching temperature and etching time as well as to determine the sensitivity of PC to neutrons.

Proton tracks on PC were created by irradiating with neutrons from the Cf-252 for 1 day. The maximum thermal neutron flux of about  $5 \times 10^4$  n/cm<sup>2</sup>.s in water from the source. Twenty four pieces of PC chips were put into an aluminum box and placed 1 cm from the Cf-252 source in order to obtain the maximum neutron flux (as illustrated in Figure 4.8). The selected etchant was still PEW solution using etching temperatures varied from 65, 70 and 75°C and etching times varied from 15, 30, 45, 60 and 90 minute (min). After etching, the recoil proton tracks were observed under an optical microscope with magnification of X100. The track density and track diameter were then analyzed by using the ImageJ software. Finally, light transmission through the track-etched PC was measured by using the SPECTRUM DETECTIVE Transmission Meter SD2400. The results are shown in Table 4.4. The results indicated that at etching temperature 80°C, track density decreased and track size increased due to too high temperature.

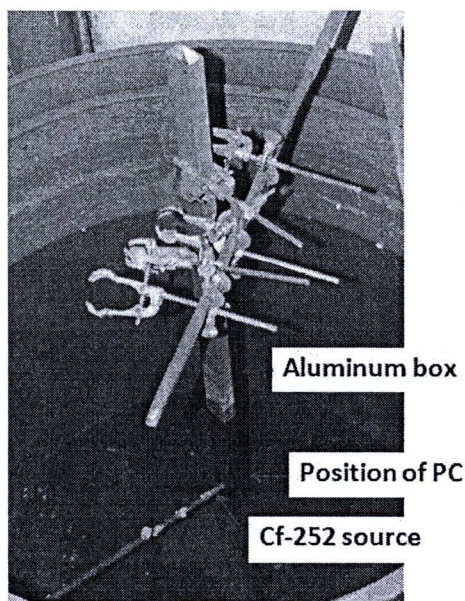


Figure 4.8 Cf-252 neutron irradiation facility.

Figures 4.9 - 4.10 illustrate the images of proton tracks on PC chips at different etching times at 65°C etching temperature. Figure 4.9 shows track images on the front

side of the PC chips (closer to Cf-252 source) while Figure 4.10 shows track images on the reverse side.

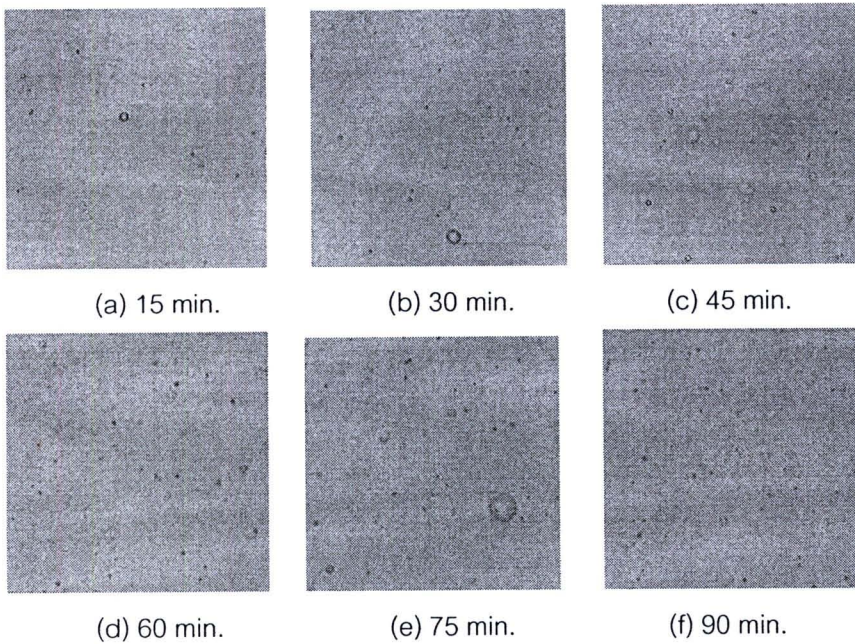


Figure 4.9 Track images (x100) on the front side of PC at different etching times and etching temperature  $65^{\circ}\text{C}$ .

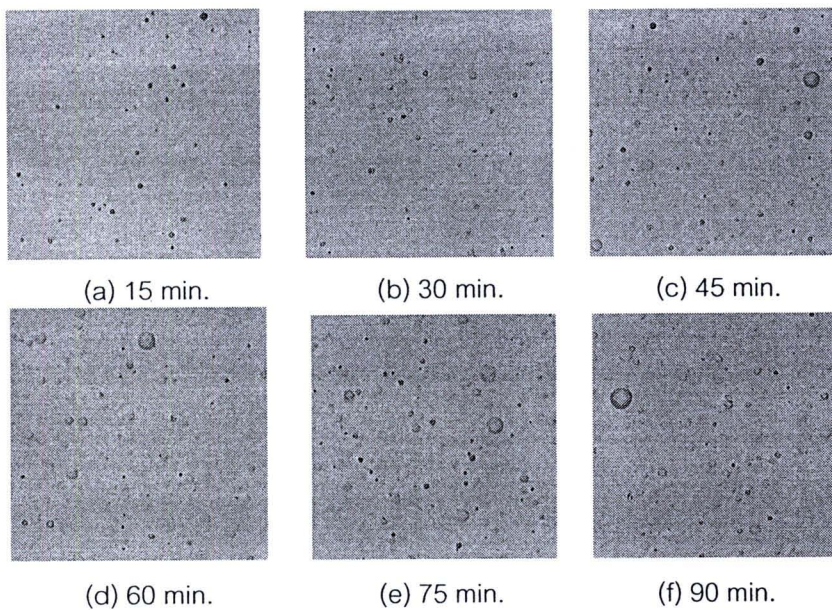


Figure 4.10 Track images (x100) on the reverse side of PC at different etching times and etching temperature  $65^{\circ}\text{C}$ .

Figures 4.11 - 4.12 illustrate the images of proton tracks on PC chips at different etching times at 70°C etching temperature. Figure 4.11 shows track images on the front side of the PC chips (closer to Cf-252 source) while Figure 4.12 shows track images on the reverse side.

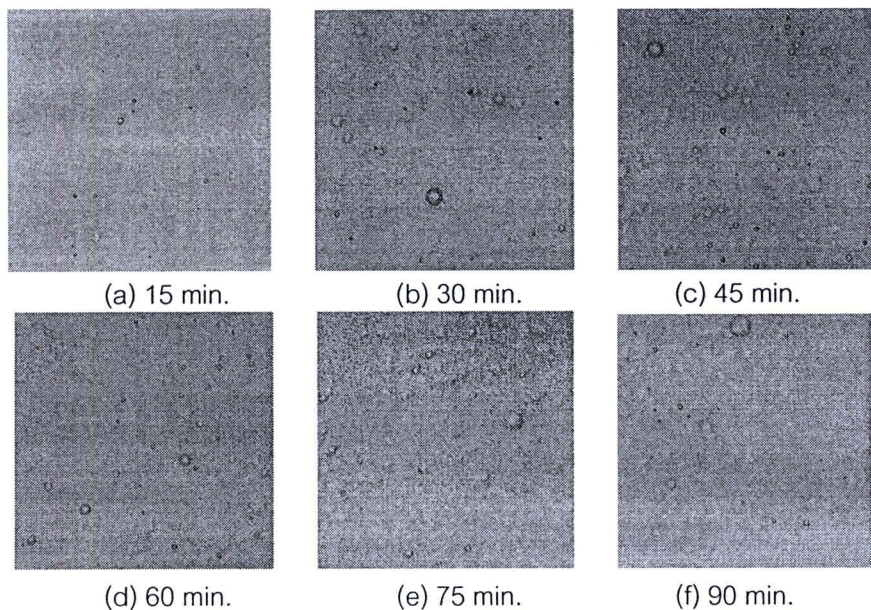


Figure 4.11 Track images (x100) on the front side of PC at different etching times and etching temperature 70°C.

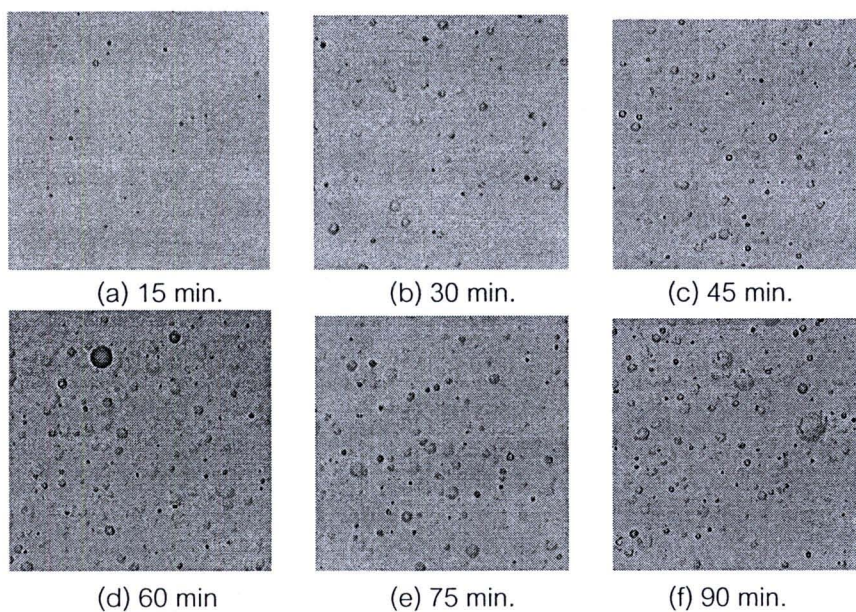


Figure 4.12 Track images (x100) on the reverse side of PC at different etching times and etching temperature 70°C.

Figures 4.13 - 4.14 illustrate the images of proton tracks on PC chips at different etching times at 75°C etching temperature. Figure 4.13 shows track images on the front side of the PC chips (closer to Cf-252 source) while Figure 4.14 shows track images on the reverse side.

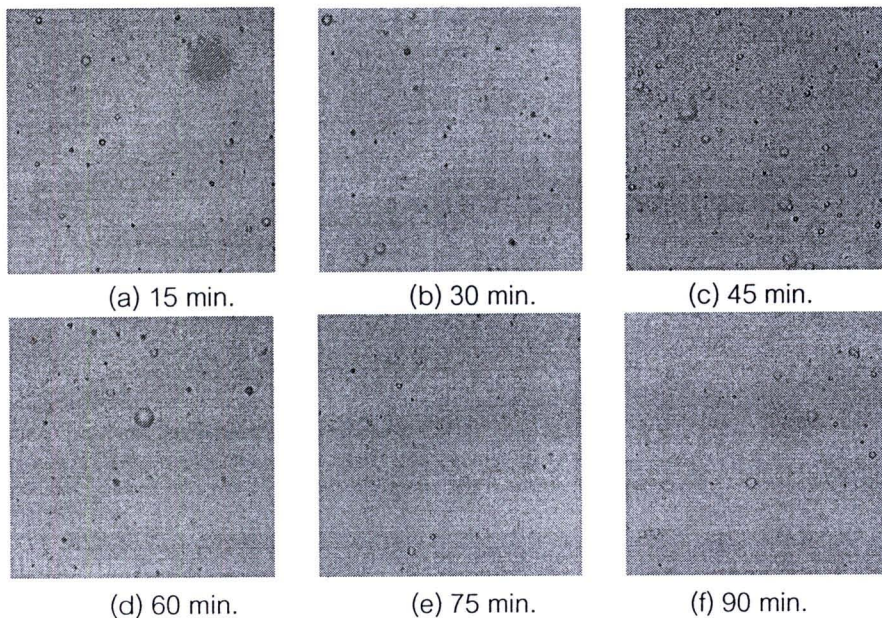


Figure 4.13 Track images (x100) on the front side of PC at different etching times and etching temperature 75°C.

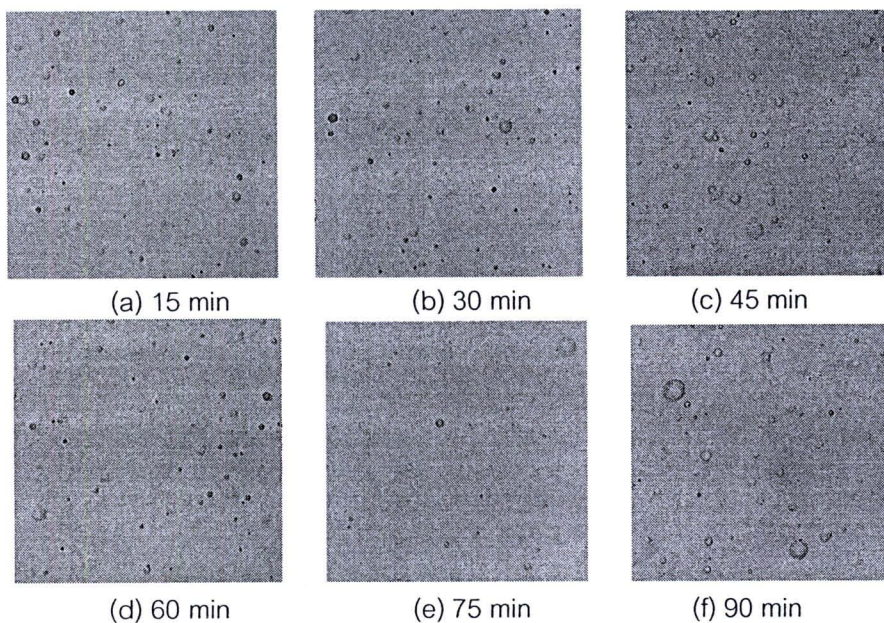


Figure 4.14 Track images (x100) on the reverse side of PC at different etching times and etching temperature 75°C.

Track densities were observed and counted on both sides of each PC chip. The track densities shown in Table 4.5 and Figure 4.15 are the total track density on both sides of the chip.

Table 4.5 Track density at different etching times and etching temperatures

Etching time	Track density (tracks/ cm <sup>2</sup> )		
	65°C	70°C	75°C
15	$1.52 \times 10^5$	$2.44 \times 10^5$	$2.86 \times 10^5$
30	$2.31 \times 10^5$	$3.26 \times 10^5$	$3.60 \times 10^5$
45	$3.08 \times 10^5$	$3.84 \times 10^5$	$4.12 \times 10^5$
60	$3.41 \times 10^5$	$4.21 \times 10^5$	$3.01 \times 10^5$
75	$3.85 \times 10^5$	$2.77 \times 10^5$	$2.37 \times 10^5$
90	$3.87 \times 10^5$	$3.24 \times 10^5$	$2.57 \times 10^5$

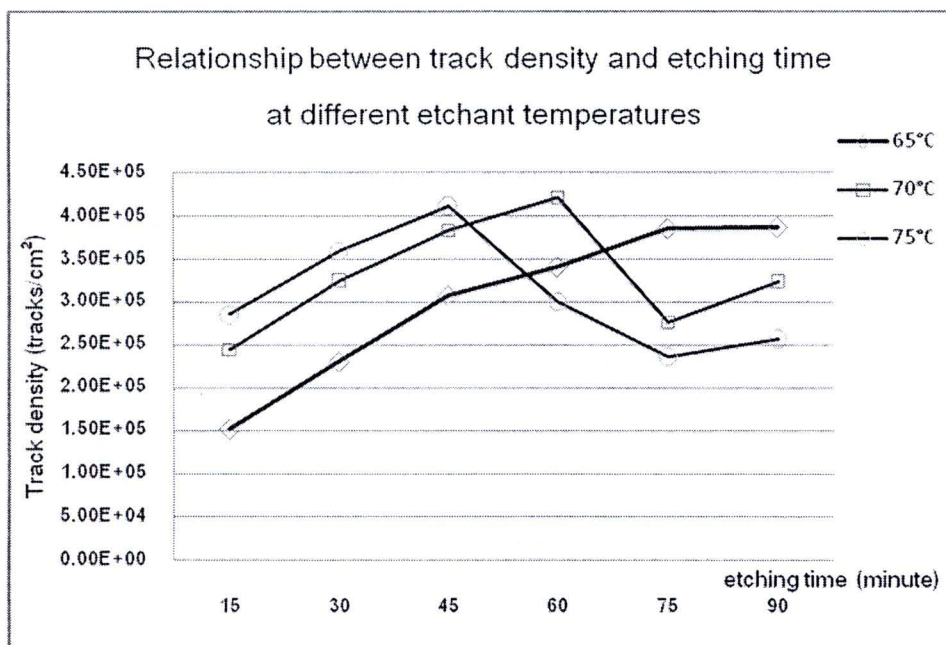


Figure 4.15 Relationship between track density and etching time at different temperatures: 65, 70 and 75°C.

The results showed that the optimum etching times for the maximum track densities at etching temperatures 65, 70 and 75°C were 75, 60 and 45 minutes respectively. At etching temperature of 70 and 75°C, the track densities increase with increasing of the etching time up to the maximum values then level off. For prolong etching time, the tracks on the surface were gradually removed resulting in decrease in track density.

Tables 4.6 - 4.8 shows distribution of track diameter at etching temperatures 65, 70 and 75 °C respectively.

Table 4.6 Distribution of track diameter at etching temperature 65 °C

Track size ( $\mu\text{m}$ )	Number of track in percentage					
	15 min	30 min	45 min	60 min	75 min	90 min
1	3.92	5.77	2.38	0.00	0.76	2.61
2	21.57	15.38	11.90	12.93	10.98	8.96
3	31.37	17.95	13.33	16.38	19.32	9.33
4	18.63	16.03	14.76	18.53	17.42	18.66
5	12.75	10.90	16.19	15.95	13.26	13.06
6	8.82	10.26	15.24	12.93	12.12	9.70
7	1.96	8.33	6.67	9.05	6.82	7.09
8	0.00	5.77	6.67	6.03	8.33	9.33
9	0.98	6.41	2.86	3.45	4.55	7.09
10	0.00	1.92	2.86	0.43	3.03	3.73
11	0.00	0.00	3.33	1.72	0.38	3.36
12	0.00	0.64	0.95	0.43	0.76	2.24
13	0.00	0.00	1.43	0.86	0.38	1.87
14	0.00	0.00	0.48	0.43	0.00	0.37
15	0.00	0.00	0.48	0.00	0.38	0.75
16	0.00	0.00	0.00	0.43	0.00	0.00
17	0.00	0.00	0.00	0.00	0.76	0.75
18	0.00	0.64	0.48	0.43	0.76	1.12
>19	3.92	5.77	2.38	0.00	0.76	2.61

Table 4.7 Distribution of track diameter at etching temperature 70 °C

Track size ( $\mu\text{m}$ )	Number of track in percentage					
	15 min	30 min	45 min	60 min	75 min	90 min
1	0.00	0.00	0.00	0.00	0.50	0.00
2	6.10	3.96	4.17	6.78	2.51	4.66
3	19.51	10.13	12.88	13.22	9.55	14.83
4	12.20	10.57	10.23	13.90	13.07	13.14
5	18.90	13.66	12.12	10.85	7.54	13.56
6	10.37	9.69	7.20	11.86	15.58	10.17
7	10.98	10.57	10.23	7.46	9.55	7.20
8	10.98	9.25	9.09	7.12	8.04	9.75
9	3.05	6.17	11.36	7.80	7.54	5.08
10	3.66	7.05	6.06	5.42	9.05	5.51
11	3.66	4.85	4.92	3.39	2.51	2.54
12	0.61	3.96	5.30	4.07	5.03	2.97
13	0.00	4.41	3.03	2.03	2.51	1.69
14	0.00	2.20	1.14	2.03	0.50	1.27
15	0.00	1.32	0.76	1.02	2.51	0.85
16	0.00	0.88	0.38	1.02	0.50	0.85
17	0.00	0.88	0.76	0.68	0.50	1.27
18	0.00	0.44	0.00	0.00	1.51	0.42
19	0.00	0.00	0.38	0.34	0.00	0.85
>20	0.00	0.00	0.00	1.02	1.51	3.39

Table 4.8 Distribution of track diameter at etching temperature 75 °C

Track size ( $\mu\text{m}$ )	Number of track in percentage					
	15 min	30 min	45 min	60 min	75 min	90 min
1	0.00	0.81	0.00	0.00	0.00	0.00
2	2.60	8.54	8.13	1.46	4.42	2.67
3	24.48	17.89	21.55	20.87	17.13	6.95
4	14.06	14.23	13.43	20.39	9.39	7.49
5	10.42	15.85	6.71	13.59	4.97	8.56
6	19.27	11.79	7.42	6.80	4.42	13.37
7	10.94	8.13	10.25	10.19	2.76	8.02
8	7.81	6.91	10.95	7.28	9.39	11.76
9	5.21	3.66	3.89	4.37	6.63	8.02
10	3.65	2.85	3.53	5.83	5.52	3.74
11	1.04	3.25	4.24	3.40	8.84	4.81
12	0.52	3.25	1.41	1.94	6.08	4.81
13	0.00	0.81	1.77	0.49	6.63	5.35
14	0.00	0.41	4.59	1.46	1.66	6.95
15	0.00	0.81	1.06	0.00	2.76	3.21
16	0.00	0.00	0.35	0.49	1.10	0.53
17	0.00	0.41	0.00	0.49	1.66	1.60
18	0.00	0.00	0.35	0.49	0.55	1.07
19	0.00	0.00	0.35	0.00	2.21	0.53
>20	0.00	0.41	0.00	0.49	3.87	0.53

Figures 4.16 - 4.18 illustrate distribution track diameter in percentage at different etching times and etching temperatures of 65, 70 and 75 °C, respectively.

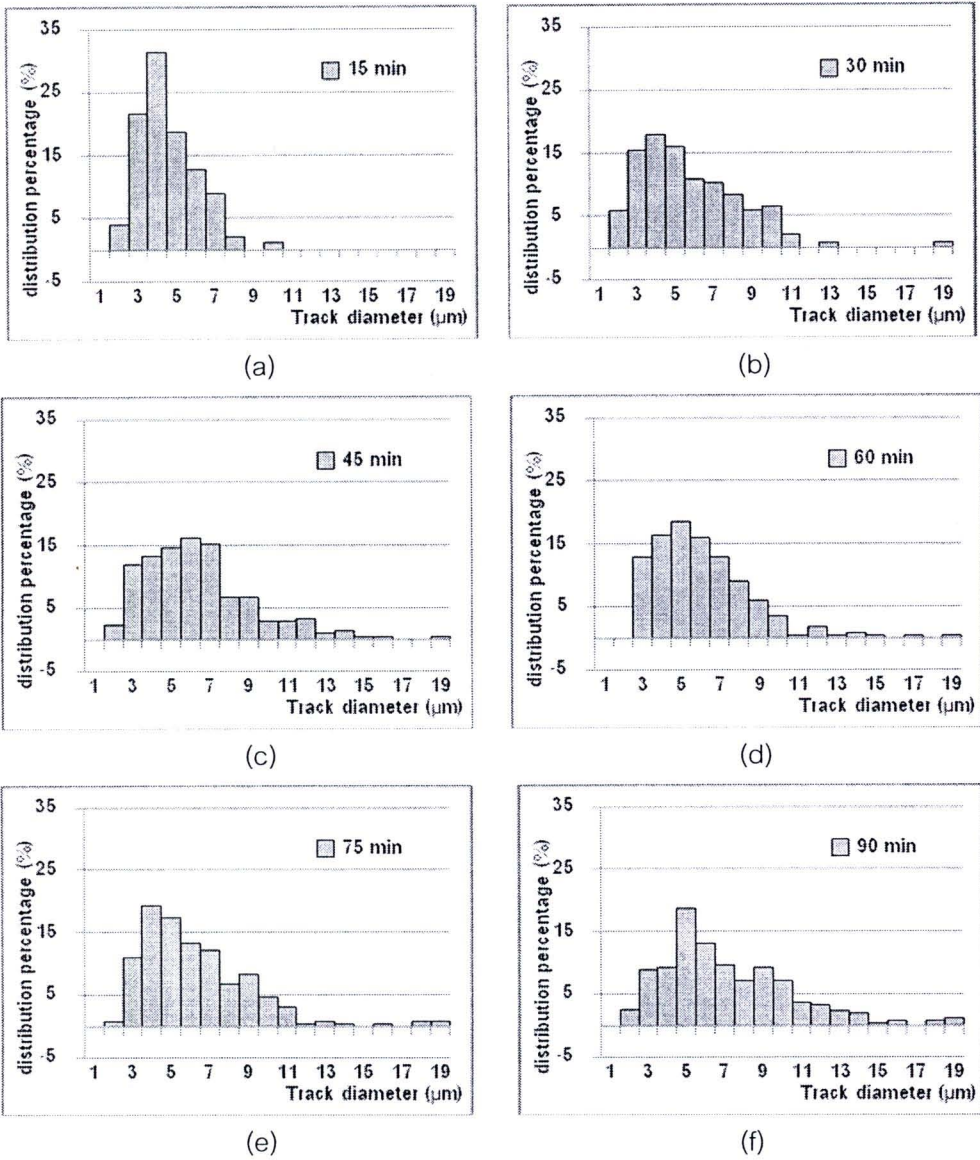


Figure 4.16 Distribution of track diameter at  $65^{\circ}\text{C}$  for different etching times.

Figure 4.16 (a) demonstrated that track diameter in shorter etching time distributed in small diameter. It was a conical phase of etching period. For the etching time 15 min, track diameter distributed in 3-5  $\mu\text{m}$  and no track diameter was larger than 10  $\mu\text{m}$ . When etching time increased, track diameter was larger due to prolonged etching time led to transitional and spherical phase [8].

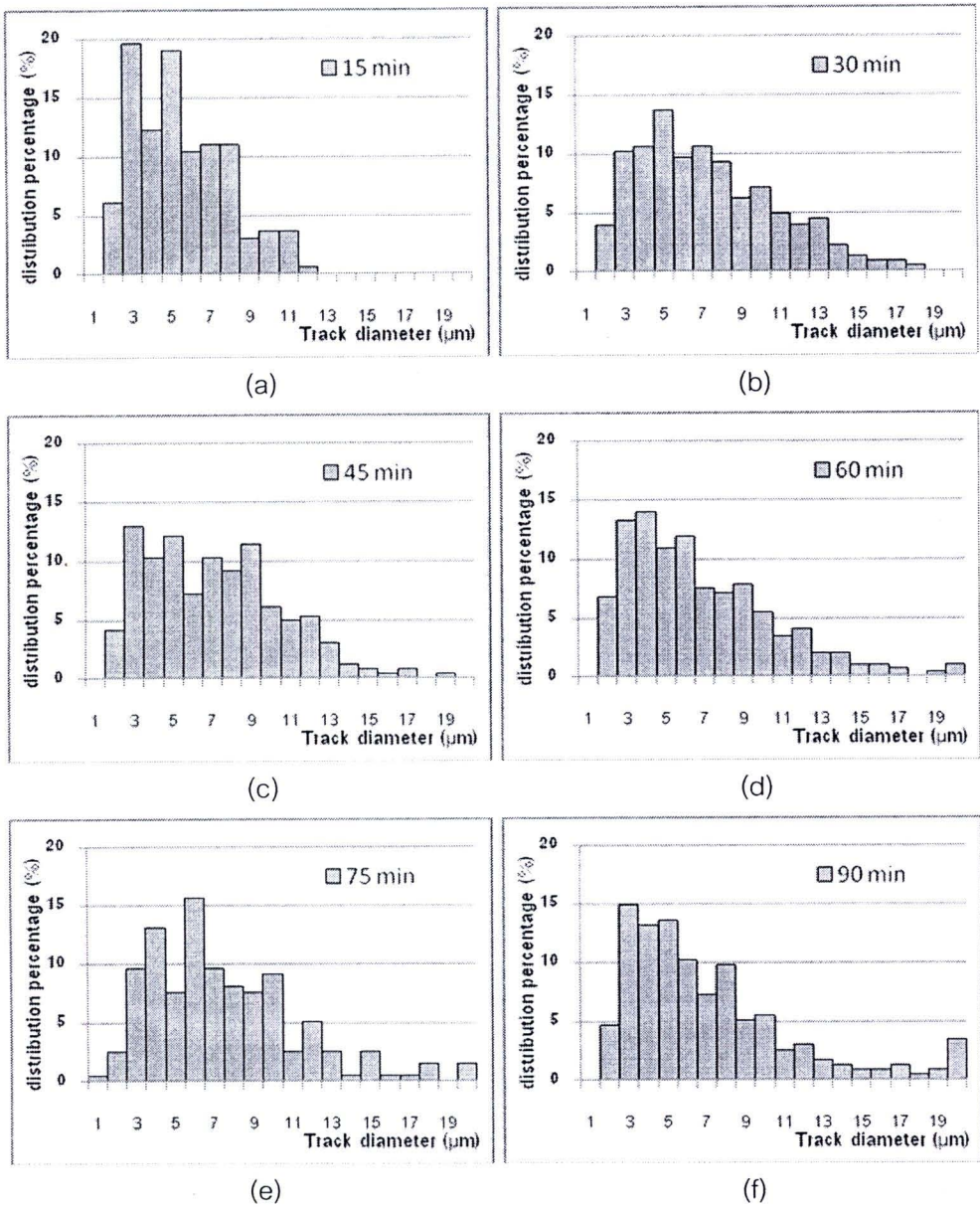


Figure 4.17 Distribution of track diameter at 70°C for different etching times.

At etchant temperature 70°C, etching time 15 min, track diameter distributed to larger size than etchant temperature 65°C, etching time 15 min. Mean of track diameter was also larger. The distribution of track diameter in other etching times distributed randomly. When etching time increased, track diameter increased.

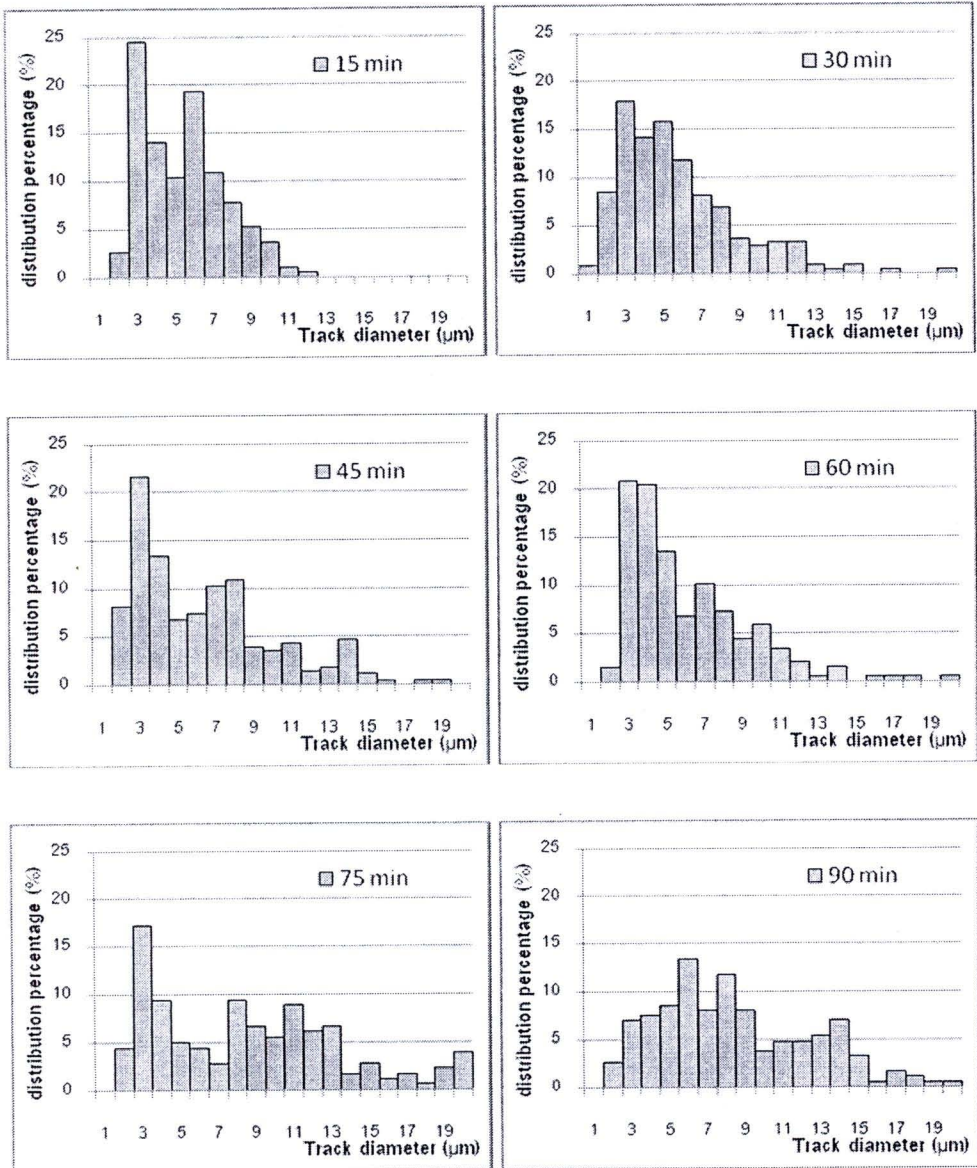


Figure 4.18 Distribution of track diameter at 75°C for different etching times.

Pattern of distribution of track diameter at 75°C at etching time 15 min was same as at 70°C. When etching time increased, track diameter distributed to larger size too. But distribution of track diameter at etching time 45 and 60 min were shifted to the smaller value again due to some of new proton tracks in the PC was observed.

Table 4.9 -4.11 showed the mean, median, standard deviation (SD), minimum and maximum values of track diameter in each etching time at etchant temperature 65, 70 and 75 °C, respectively.

Table 4.9 Statistic values of track diameter in each etching time at 65°C

Etching time (min)	Track diameter ( $\mu\text{m}$ )				
	Mean	Median	SD	Minimum	Maximum
15	5.01	4.57	1.49	2.19	10.32
30	6.17	5.69	2.64	2.19	19.75
45	6.92	6.66	3.10	2.31	25.66
60	7.00	6.23	2.57	3.02	19.29
75	6.79	6.08	3.19	2.43	31.63
90	7.57	6.62	3.39	2.19	19.57

Table 4.10 Statistic values of track diameter in each etching time at 70°C

Etching time (min)	Track diameter ( $\mu\text{m}$ )				
	Mean	Median	SD	Minimum	Maximum
15	6.02	5.59	2.39	2.31	12.17
30	7.78	7.28	3.53	2.53	18.70
45	7.59	7.28	3.41	2.19	19.72
60	7.32	6.50	3.80	2.19	24.88
75	7.96	7.05	4.74	1.64	23.20
90	7.72	6.35	3.81	2.19	32.13

Table 4.11 Statistic values of track diameter in each etching time at 75°C

Etching time (min)	Track diameter ( $\mu\text{m}$ )				
	Mean	Median	SD	Minimum	Maximum
15	5.91	5.71	2.26	2.07	12.33
30	6.20	5.47	3.14	1.94	22.47
45	6.79	6.25	3.19	2.31	19.90
60	6.55	5.47	3.46	2.64	29.76
75	9.12	8.78	5.11	2.31	27.17
90	8.93	8.47	4.03	2.31	22.07

The mean and median of track diameter at 65 and 70°C in each etching time were not different significant. But Mean and median of track diameter at 75°C in each etching time were different significant.

Table 4.12 showed percentage of light transmission at the different temperature. All of track-etched PCs were decreased visible and IR transmissions compare to control PC with etching and control without etching and with neutron irradiation. UV was absorbed by thickness of PC. The transmission of visible light and IR at shorter etching time was less effect than longer etching time. Those mean the distribution of track diameter affect the transmission of visible light and IR. The results showed that PC with variation of distribution of track diameter affect the transmission of light and IR.

Table 4.12 Percentage of light transmission at the different temperature

Etching time condition	Percentage of transmission (%)								
	65°C			70°C			75°C		
	UV	Visible light	IR	UV	Visible light	IR	UV	Visible light	IR
No PC	100	100	100	100	100	100	100	100	100
C <sub>no etch</sub>	0	85	92	0	85	92	0	85	92
C <sub>etch 90 min</sub>	0	84	91	0	84	92	0	84	92
15 min	0	83	91	0	82	89	0	83	91
30 min	0	82	90	0	82	88	0	82	90
45 min	0	81	89	0	82	88	0	81	88
60 min	0	80	88	0	80	87	0	81	89
75 min	0	80	88	0	80	87	0	80	88
90 min	0	80	88	0	80	87	0	80	87

Note: C<sub>no etch</sub> no etch was control PC without etching

C<sub>etch</sub> was control PC with etching for 90 min

The transmission of UV through all of PCs was totally absorbed by inherent properties of PC. Shorter etching time led to less track density and distribution of smaller track diameter, it will not affect the transmission of visible light and IR. The distribution within larger diameter and larger track density will increase the effect of transmission of visible light and IR. But they were not different significant.

From the above data of track density, distribution percentage of track diameter and percentage of light transmission in each temperature was found that proton track on PC affected percentage of visible light and infrared transmission.

#### 4.2.2 Variation condition of tracked-etch PC

Track-etched PC was formed in different condition of track density, etching time and etchant temperature in order to correlate with transmission of light. The condition of PC was divided into six conditions following as Table 4.13 to form the different track size, shape (Figure 4.19) and track density (Table 4.14). In this study, track density and size were analyzed only reverse side of PC.

Table 4.13 Condition of neutron irradiation, etchant temperature and etching time

	irradiation time	PEW(°C)	etching time
condition 1	3 days	75	15 min
condition 2	3 days	70	15 min
condition 3	3 days	65	30 min
condition 4	7 days	70	45 min
condition 5	3 days	70	35 min
condition 6	7 days	70	60 min

Table 4.14 Track densities in various conditions

Condition	Track density on one side (tracks/ cm <sup>2</sup> )	Sensitivity in formation of proton tracks*
1	$3.04 \times 10^5$	$2.3 \times 10^{-5}$
2	$3.74 \times 10^5$	$2.9 \times 10^{-5}$
3	$3.85 \times 10^5$	$3.0 \times 10^{-5}$
4	$5.39 \times 10^5$	$1.8 \times 10^{-5}$
5	$5.83 \times 10^5$	$4.5 \times 10^{-5}$
6	$1.11 \times 10^6$	$3.7 \times 10^{-5}$

\* = obtained from track density (tracks/cm<sup>2</sup>) divided by neutron fluence (n/cm<sup>2</sup>)

Track density on PC condition 4 and 5 was more than condition 1-3 about 1 time and condition 6 was more than condition 1-3 about 2 times .

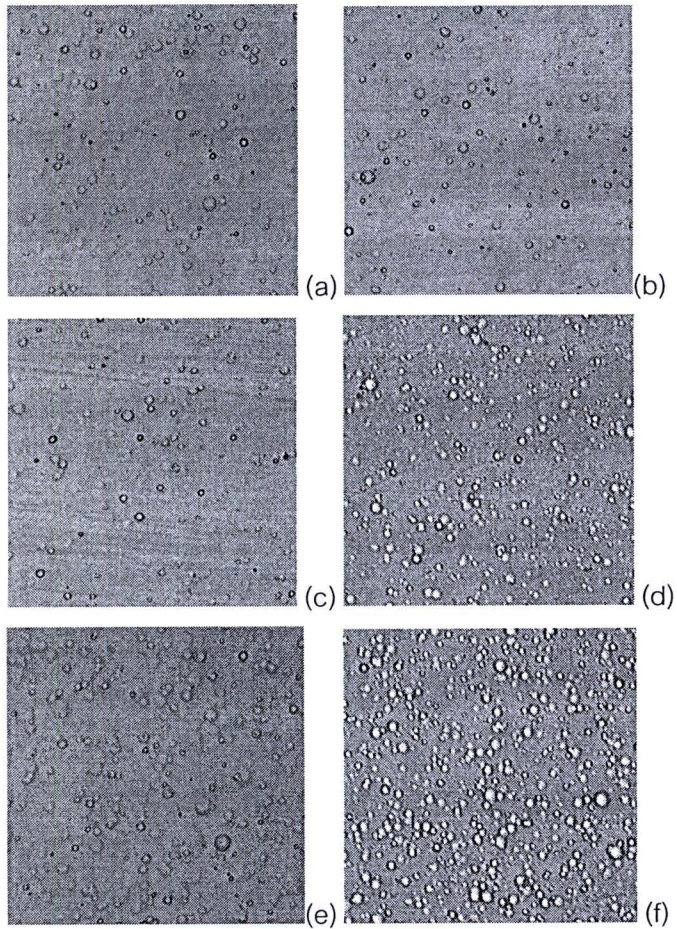


Figure 4.19 Capture track image (400x400 pixels) on the reverse side in various conditions (a) condition 1, (b) condition 2, (c) condition 3, (d) condition 4, (e) condition 5 and (f) condition 6.

The distribution percentage of track diameter was shown in Table 4.15 and plotted curve shown as Figure 4.20. Table 4.16 showed the mean, median, standard deviation (SD), minimum and maximum values of track diameter in each condition.

Table 4.15 Distribution of track diameter at different conditions

Track size ( $\mu\text{m}$ )	Number of track in percentage (%)					
	Condition 1	Condition 2	Condition 3	Condition 4	Condition 5	Condition 6
1	0.00	0.00	0.00	0.00	0.00	0.00
2	1.48	4.38	0.78	0.83	3.05	0.00
3	1.48	8.37	5.04	1.94	14.97	0.27
4	6.40	10.76	8.53	4.43	16.50	2.68
5	10.84	14.34	23.26	24.38	16.50	11.54
6	12.32	14.74	21.71	29.92	12.94	27.92
7	14.78	17.13	15.50	18.01	12.18	25.64
8	18.23	14.34	13.57	9.97	11.17	15.44
9	13.79	7.97	8.14	6.37	4.82	8.05
10	8.37	5.58	2.71	2.77	2.79	4.56
11	6.90	1.59	0.78	0.83	3.30	2.55
12	1.48	0.80	0.00	0.55	0.51	0.81
13	1.48	0.00	0.00	0.00	0.51	0.27
14	2.46	0.00	0.00	0.00	0.25	0.00
15	0.00	0.00	0.00	0.00	0.25	0.27
16	0.00	0.00	0.00	0.00	0.25	0.00

Table 4.16 Statistic values of track diameter in each conditions

Condition	Track diameter ( $\mu\text{m}$ )				
	Mean	Median	SD	Minimum	Maximum
1	8.13	8.04	2.44	2.74	14.84
2	6.76	6.78	2.21	2.31	12.77
3	6.71	6.58	1.82	1.03	12.52
4	7.81	7.51	1.64	1.03	13.31
5	6.35	5.94	2.46	2.19	16.61
6	7.53	6.50	1.65	3.10	15.97

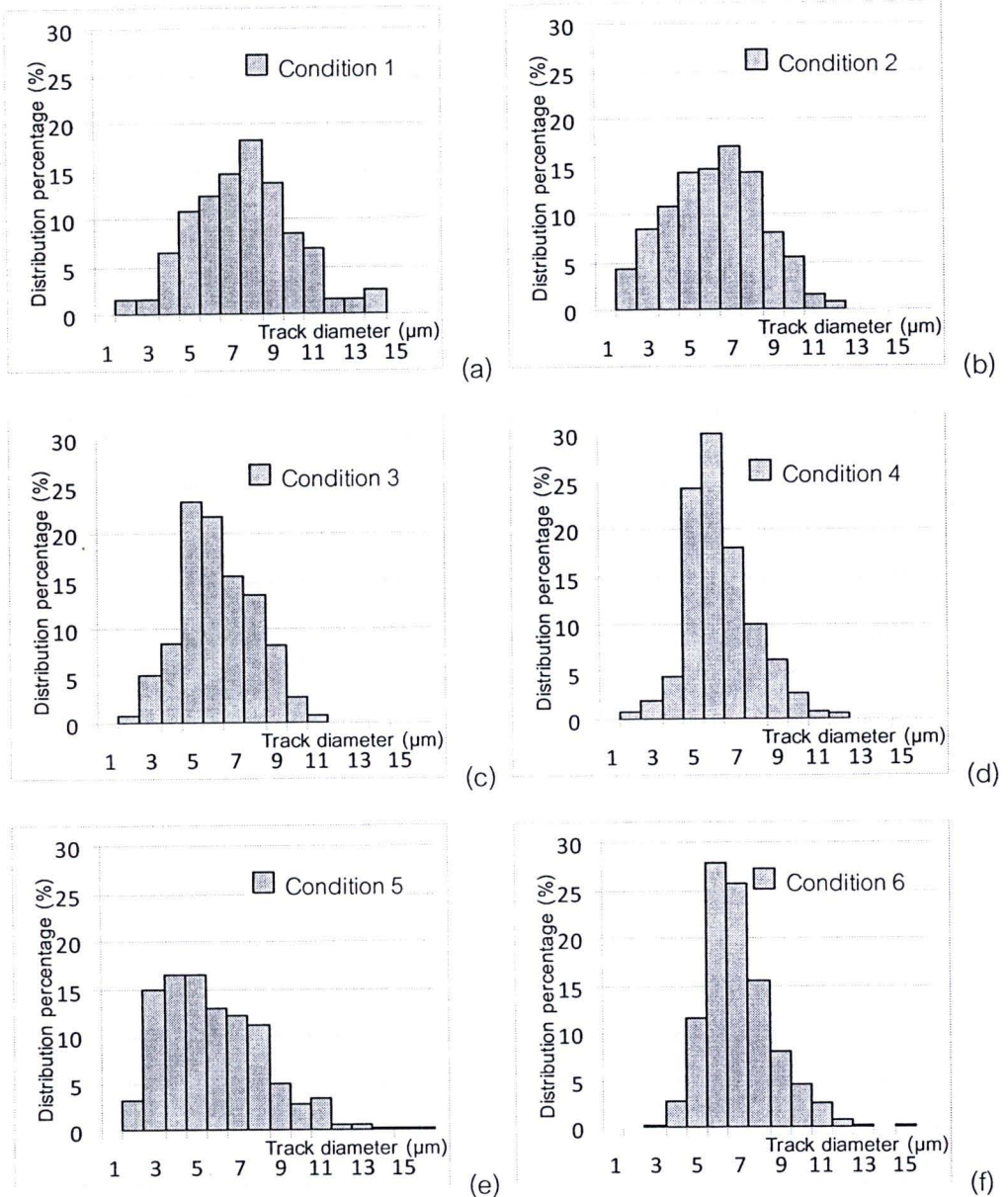


Figure 4.20 Distribution of track diameter for different conditions.

From Table 4.14 and Figure 4.20 showed that track density and distribution of track diameter in each condition were different. The distribution percentage of track diameter can be divided into two patterns. First pattern was condition 1, 2 and 5. Track diameters were distributed randomly in wide range of diameter. Their standard deviations were 2.44, 2.21 and 2.46, respectively. Second pattern was condition 3, 4 and 6. Distribution of diameter in each condition was different from first pattern. It varied within narrow range of track diameter. Their standard deviations were 1.82, 1.64 and 1.65, respectively.

Table 4.17 showed percentage of transmission of UV, visible light and IR through the different track-etched PCs.

Table 4.17 Percentage of light transmission at different conditions

	Percentage of transmission (%)								
	no PC	C <sub>no etch</sub>	C <sub>etch</sub>	#1	#2	#3	#4	#5	#6
UV	100	0	0	0	0	0	0	0	0
Light	100	85	84	81	79	80	81	77	72
IR	100	91	91	88	86	88	90	84	80

The results showed that UV was absorbed by all of PCs. The minimum and maximum effects of track-etched PCs to percentage of light and IR transmission were condition 4 and 6, respectively. This study showed that the different track density and different distribution of track diameter affected percentage of light and IR transmission. Larger of track density and distribution of track diameter within wide range increased the effect of transmission of visible light and IR.

The simplified experiment on transmission of laser pointer beam was set to observe the effect of laser light transmission (Figure 4.21). The wavelength of laser pointer was 650-670 nanometer (nm). Figure 4.22 displayed the projected image of laser pointer beam transmitted through track-etched PC.

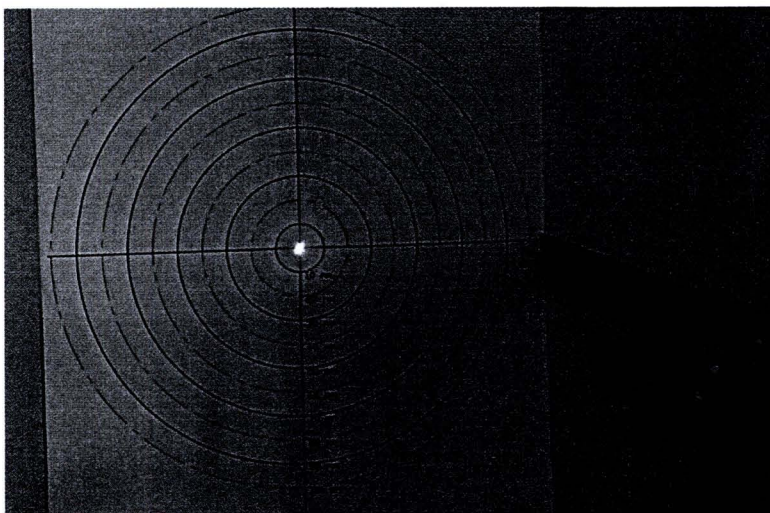


Figure 4.21 Setting of experiment on transmission of laser beam from laser pointer.

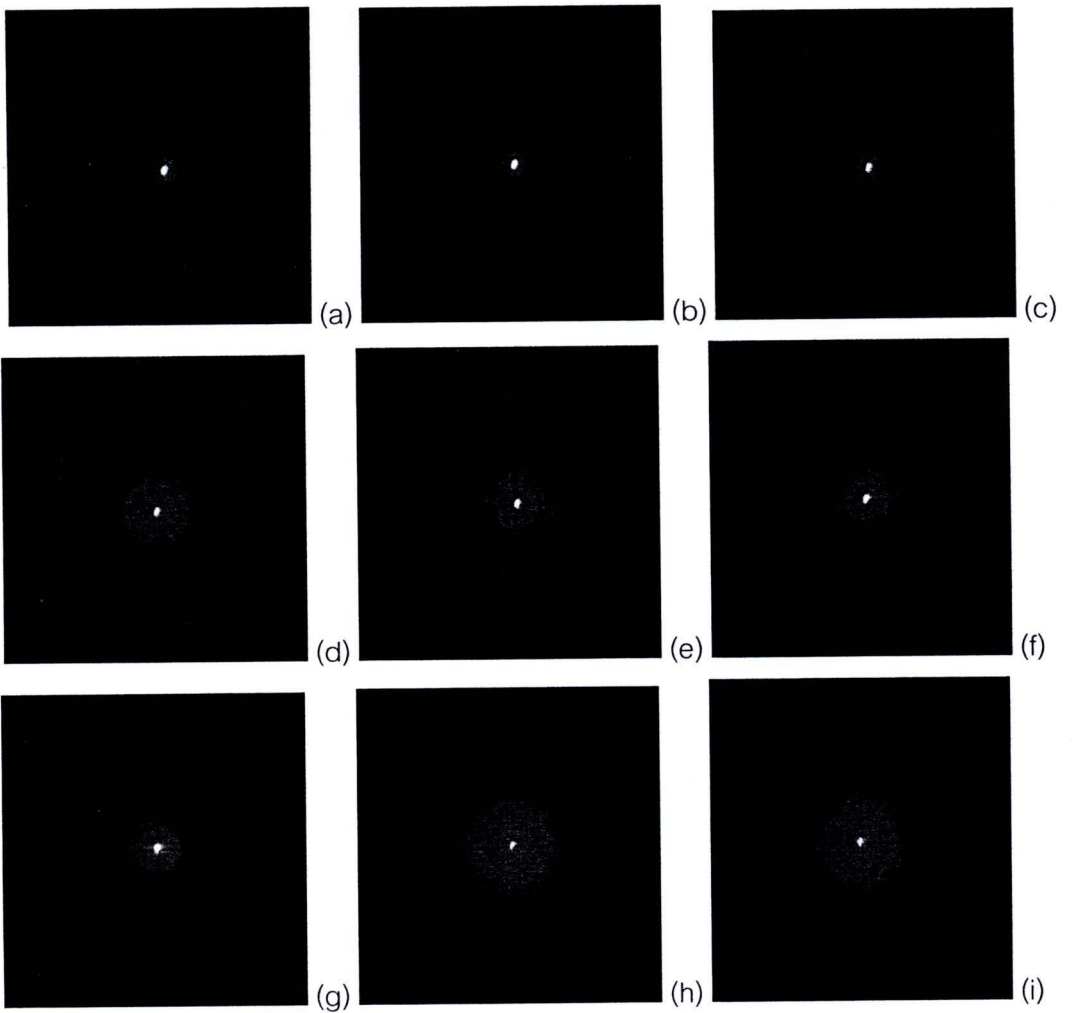


Figure 4.22 Projected image of laser pointer beam transmitted through track-etched PC in various conditions: (a) No PC, (b) PC with etching, (c) PC with neutron irradiation, without etching, (d) condition 1, (e) condition 2, (f) condition 3, (g) condition 4, (h) condition 5 and (i) condition 6.

Projected images of laser pointer beam transmitted through track-etched PC in various conditions were analyzed by using plot profile of ImageJ software in order to change to intensity profile. It was shown as Figure 4.23.

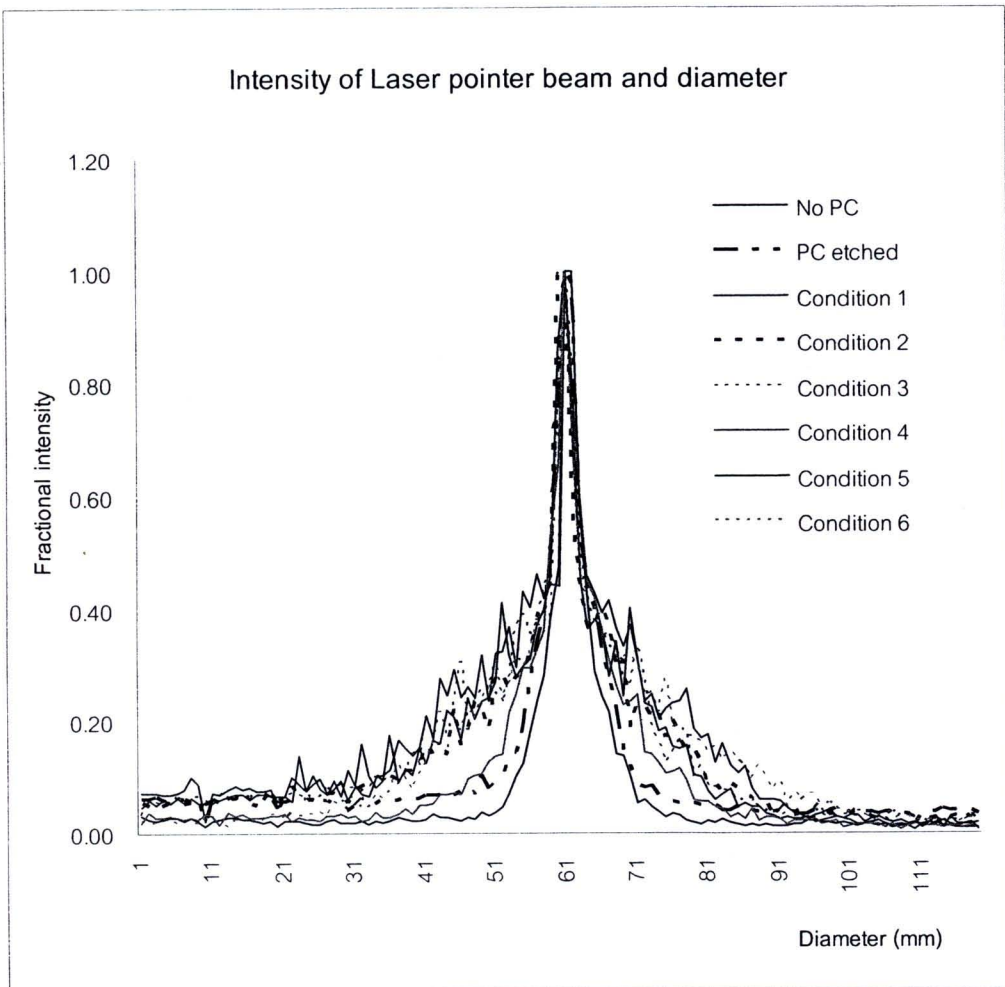


Figure 4.23 Intensity profile of projected image of laser pointer beam transmitted through track-etched PC in various conditions.

The results showed that the projected image of laser beam transmission was related to the percentage of IR transmission in table 4.10. Projected image of laser beam of No PC, PC with etching condition were not different. PC with condition 5 and 6 diffused laser pointer beam more than the condition of No PC and PC with etching about 3 times. The minimum diffusion effect of laser pointer beam was PC in condition 4. The result corresponded with the percentage of IR transmission.

#### 4.2.3 Reproducibility test

The reproducibility test was performed by comparing analysis data of three track-etched PCs irradiated and etched with the same condition in terms of track density, track diameter distribution, mean, median, SD of track diameter and

neutron from Cf-252 source 1day and etched PEW solution at etchant temperature 70°C, 1 hr. The analyzed data were shown in Figure 4.24 and Table 4.18.

Table 4.18 Comparison data of Track density, mean, median, SD and transmission percentage of UV, visible light and IR

	PC no. 1	PC no. 2	PC no. 3
Track density (tracks/cm <sup>2</sup> )	3.99 x 10 <sup>5</sup>	4.08 x 10 <sup>5</sup>	4.11 x 10 <sup>5</sup>
Mean (µm)	7.27	7.21	6.97
Median (µm)	6.54	6.33	6.25
SD	3.11	3.33	2.87
Minimum	1.94	2.19	2.83
Maximum	19.56	20.56	19.22
Transmission percentage of			
- Ultraviolet	0	0	0
- visible light	84	84	84
- Infrared	87	86	87

The results showed that track density, mean and median of track diameter of track-etched PC no. 3 differed from track-etched PC no. 1 and 2 less than 5%. Transmission of UV, visible light and IR of all conditions were not different significant.

Figure 4.24 showed that most probability of track diameter of all track-etched PCs were 5 µm. Distribution of track diameter of track-etched PC no. 1 and 2 were same patterns but track diameter of track-etched PC no. 3 distributed mild differently.

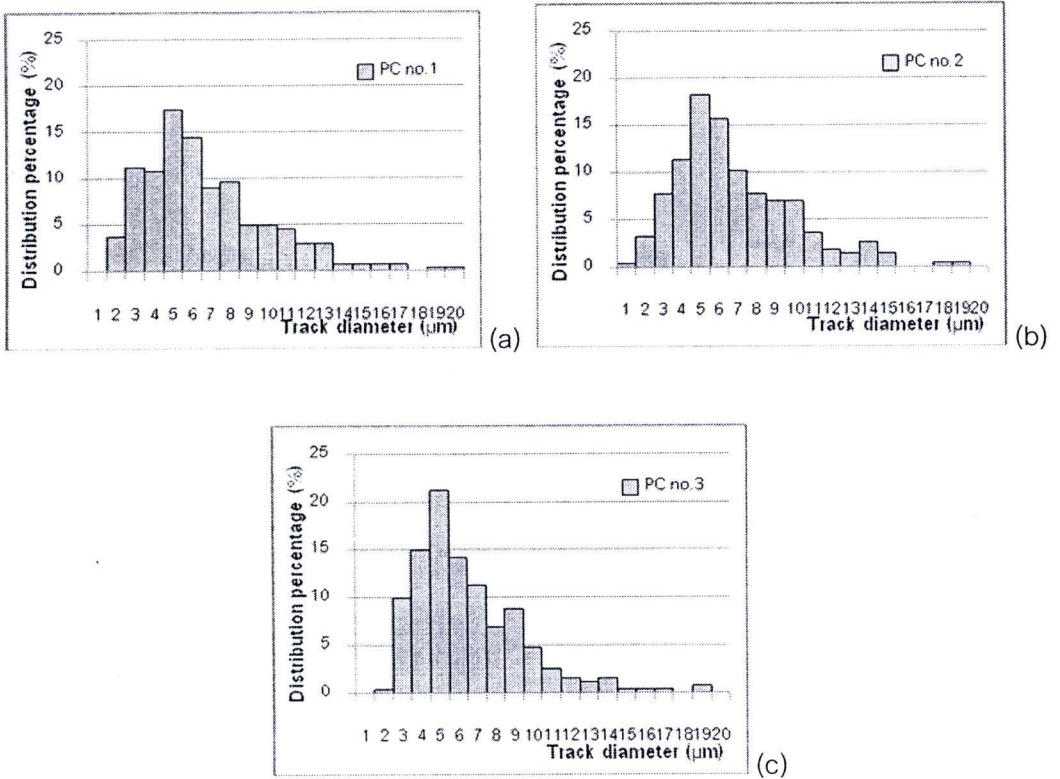


Figure 4.24 Distribution of track diameter of track-etched PC no.1, 2 and 3 with neutron irradiation time 1 day, etched PEW 70°C, 1 hr.

#### 4.3 Physical properties test of track-etched PC

In this study, two pieces of track-etched PC, PC with etching and original PC chips were tested physical properties in terms of tension and impact strength tests in order to observe the difference. Tension strength was tested by Scientific and Technological Research Equipment Center, Chulalongkorn University and impact strength was done by Department of Science service, Bangkok, Thailand. The test reports were shown in Appendix F. Table 4.19 showed the maximum stress of tensile strength test. The results were not different significant. In part of impact strength test, there was limitation of a hammer load of test at Department of Science service, the maximum load was 22 J. the results showed the impact strength of all of PC conditions were bigger than 22 J or 150 J/cm<sup>2</sup>.

Table 4.19 Tensile strength test

PC conditions	Tensile strength test: Maximum Stress (kgf/mm <sup>2</sup> )
<b>Original PC:</b>	
Piece no. 1	5.15
Piece no. 2	6.41
<b>PC with etched 1 hr:</b>	
Piece no: 1	6.32
Piece no. 2	6.35
<b>PC with neutron irradiated 3 day and etched 1 hr:</b>	
Piece no. 1	6.01
Piece no. 2	5.43

#### 4.4 Design of a Cf-252 neutron irradiation facility

From this investigation, it could be concluded that track-etched polycarbonate can be produced by irradiating PC chips with thermal neutrons from a Cf-252 source. However, for the source used in this research, the irradiation time about 3 days is practically too long for manufacturing track-etched PC. The source used in this research had originally neutron emission rate of  $4.54 \times 10^7$  neutrons per second (n/s) on 28<sup>th</sup> of June 2002 as shown in Figure 3, Appendix A. The emission rate in June 2010 when the experiment was conducted the neutron emission rate was approximately  $5 \times 10^6$  n/s. The maximum neutron flux in water was therefore only about  $5 \times 10^4$  n/cm<sup>2</sup>.s which was about 100 times lower than that from the research reactor. Therefore, the Cf-252 source strength needs to be increased for production purpose. The sensitivities to neutrons in formation of recoil proton tracks at 1 cm from Cf-252 source were found to be in the range of  $1.8 \times 10^{-5}$  to  $4.5 \times 10^{-5}$  as shown in Table 4.14 which were close to the sensitivity of CR39 track-etched detector in formation of recoil proton tracks of  $1.2 \times 10^{-5}$  as claimed by G. Dajko [31].

neutron flux in water can be obtained from the thermalization factor of Cf-252 which equals 100 [32]. So, the maximum flux equals  $9.2 \times 10^8 / 100 = 9.2 \times 10^6$ . It can be also calculated by using a factor obtained from the graph for Cf-252, at a desired distance from the source, in Figure 3 in Appendix B. For example at 1 cm, the factor is  $1.1 \times 10^{-2}$  n/cm<sup>2</sup>.s per neutron emitted from the source. Thus the maximum neutron flux is about  $9.2 \times 10^8 \times 1.1 \times 10^{-2} \approx 1 \times 10^7$  n/cm<sup>2</sup>.s which is about the same as obtained from the graph and about 8 times of the neutron flux from the neutron beam for neutron radiography at the Thai Research Reactor in 4.1 (Formation of proton tracks using thermal neutrons from the Thai Research Reactor). Practically, if the irradiation position is moved further from the source, larger piece of PC can be placed around the source for neutron irradiation but the neutron flux will be decreased. For example, at 10 cm from the source neutron flux will be about  $4 \times 10^{-3} \times 9.2 \times 10^8 = 3.68 \times 10^6$  n/cm<sup>2</sup>.s which is about 3 times of the neutron flux from the neutron radiography beam port at the Thai Research Reactor. For neutron moderator apart from water (such as transformer oil, low density polyethylene or high density polyethylene), neutron flux can be further increased by a factor of 1.1 to 1.8 [32] as shown in Figure 4, Appendix A.

The irradiation time with 400 µg Cf-252 source will be greatly reduced. For example, irradiation time of 3 days is needed for the source used in this research. The irradiation time with a 400 µg Cf-252 source will be  $(5 \times 10^4 \times 3) / 3.68 \times 10^6 = 58.6$  minutes which is about 1 hour.

Figures 4.26 and 4.27 illustrate the design of neutron irradiation. Design of neutron irradiation by using Cf-252 source in water, Cf-252 source is placed in the middle of water tank. In this design, four pieces of PC sheets can be placed around the source with the distance 10 cm from the source. The other is design of neutron irradiation by using Cf-252 source in a polyethylene cube in order to increase the neutron flux. The picture shows four pieces of PC sheet are put on the windows, the other two pieces of PC sheets was put on the anterior and posterior windows.

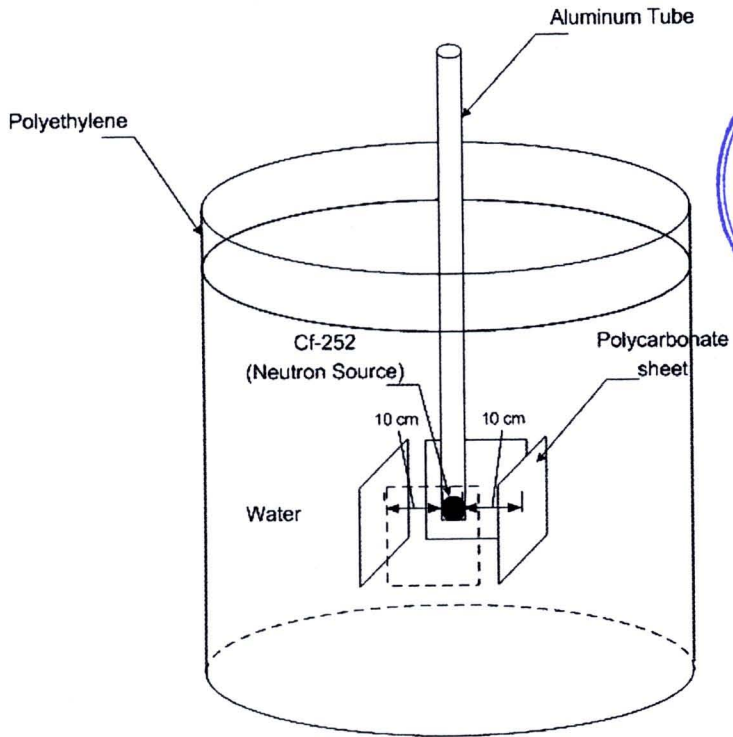


Figure 4.25 Design of neutron irradiation by using Cf-252 source in water.

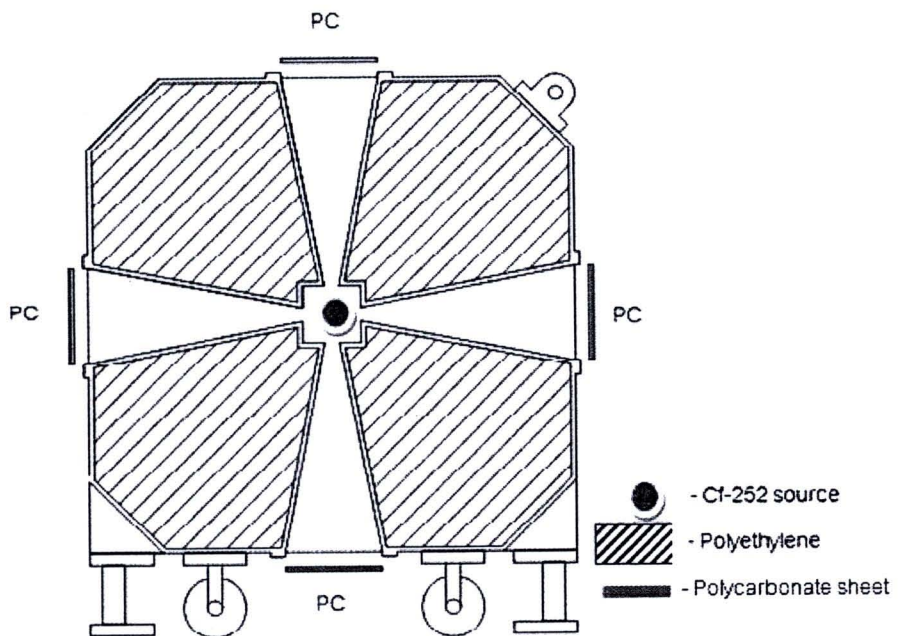


Figure 4.26 Design of neutron irradiation by using Cf-252 source in polyethylene tank.